

The dynamic simulation of the 46SiCrMo6 steel-primary suspension spring in locomotives

Muhammad Fatoni Mawarudin^a, Daryano^b, Achmad Fauzan Heri Soegiharto^c

^a Department of Mechanical Engineering, Universitas Muhammadiyah Malang
Malang, Indonesia

Email of the corresponding author: daryono@umm.ac.id

Abstract

The railway suspension system is designed to reduce vibrations and shocks that occur when a train traverses the tracks. Given the high level of vibrations experienced by trains at high speeds, it is crucial to develop an effective suspension system to mitigate these vibrations. Previous studies focused on static analysis of the locomotive's primary suspension spring. However, static stress analysis failed to reveal the cause of material failure, necessitating a dynamic analysis. This study focuses on the dynamic modelling and analysis of the primary suspension spring made of 46SiCrMo6 steel. The simulation tests were conducted using Ansys Workbench for modal and harmonic response analysis, while the geometric design of the spring was done in Inventor. The results showed that during modal analysis testing, the spring exhibited six natural frequency modes, corresponding to the train's bumping and turning conditions. The simulation of the 46SiCrMo6 steel spring indicated deformation in the middle coil, where strain occurred, leading to frequent material failure in these parts.

Keywords: 46SiCrMo6, simulation, spring, suspension

1. Introduction

The railway transportation system is the backbone of smart cities and one of the primary modes of transport in many countries worldwide [1]. This system has existed for centuries and has undergone significant developments over time. In recent decades, railway technology and speed have changed dramatically [2], as evidenced by the development and operationalization of the Jakarta-Bandung high-speed railway. This project represents a significant step in transportation infrastructure development and is expected to have a positive impact on society.

Although the use of railway public transportation is often encouraged, the travel experience is not always optimal in terms of comfort [3]. Every mode of transportation has aspects that need improvement or enhancement, and in the context of modern transportation industry development, the integration of transport systems is essential for advancing railways [4]. In some large islands or coastal regions, railways can be part of a multimodal journey involving sea transport, such as ferries or cruise ships, where this integration is crucial for long-distance freight transport.

As railway travel distances increase, the stability of high-speed trains becomes a primary objective in optimizing bogie suspension parameters [5]. When trains operate at high speeds, the frequency of external stimuli approaches the natural frequency of critical bogie components, leading to vibrations [6]. Vibrations in the bogie and wheelset can cause high levels of wheel wear [7], where the mechanical performance of the bogie directly affects the safety and comfort of train operations [8]. Short-wavelength rail corrugations induce strong vibrations in the axle boxes and bogie frames, accelerating fatigue failure in bogie components and the train frame [9].

Enhancing wheel conicity and damping can reduce unstable, low-frequency vibrations in long trains [10]. Therefore, vibration analysis is crucial to improving comfort during train operations.

Due to the high vibrations experienced during high-speed train operation, developing a suspension system to mitigate these vibrations is essential [11]. The dynamic behavior of trains heavily relies on suspensions that ensure stability and, consequently, driving safety [12]. The suspension system is designed to reduce vibrations and shocks as the train traverses the tracks, with the primary goal of enhancing passenger comfort and protecting the train structure from shock-induced damage. Therefore, the flexibility of the body and the suspension system are critical in achieving driving comfort [13]. Although many effective bogie suspension systems have been developed to improve ride comfort, certain aspects still require improvement [14]. Thus, a thorough analysis is needed to identify the most suitable suspension structure [15].

Previous studies have focused on the static analysis of the primary suspension springs in locomotives [16]. Static load analysis is used to evaluate the response of a structure to applied loads. However, this analysis has not fully revealed the causes of material failure, necessitating a dynamic analysis [17]. The material used in testing is also a critical factor.

The current study involves dynamic modelling and analysis of the primary suspension spring using 46SiCrMo6 steel [18]. 46SiCrMo6 steel is a high-alloy steel that meets EN 1.8065 standards, commonly used in manufacturing due to its superior mechanical properties, such as high hardness and optimal toughness after hardening and tempering processes. This material is well-suited as the primary material for train bogie springs.

Testing the spring under various field conditions, such as during turning and bumping, is crucial to understanding the material's limits. Therefore, comparisons of stress, deformation, and natural frequency of the primary spring are studied to determine the most suitable material.

2. Methods

This research conducted dynamic simulations of a primary suspension of 46SiCrMo6 steel spring for locomotive applications. It was conducted using Ansys Workbench. The mechanical properties of 46SiCrMo6 steel were defined within the data module, including Young's modulus, yield strength, and tensile strength. Meanwhile, the geometric design of the spring was created using Inventor. Several reference data points were required to conduct this research. The geometric model of helical spring dimensions was developed. Boundary conditions were applied by fixing one end of the spring and allowing vertical movement on the other, while dynamic loading conditions were simulated using time-dependent or vibration-based forces.

Table 1 presents the dimensions of the helical spring used in this study. These dimensions are crucial to ensure accuracy in the simulation and geometric design of the primary suspension spring.

Table 1. Helical Spring Dimensions

Description	Dimension
Wire Diameter (d)	33.5 mm
Outer Diameter (Do)	244.5 mm
Mean Diameter (D)	211 mm
Free Height (Hf)	360 mm
Test Load (W)	19.6 KN (per spring)
Number of Active Coils (n)	8
Pitch	63 mm

Additionally, each spring possesses specific material properties necessary for testing. In this study, three different materials were compared, one of which is 46SiCrMo6 steel, with material properties as shown in Table 2.

Table 2. Material Properties of 46SiCrMo6 Steel

Description	Dimension
Tensile Strength	1850 MPa
Yield Strength	1400 MPa
Young's Modulus (E)	200 GPa
Density (ρ)	7800 Kg/m ³
Poisson's Ratio	0.3

In this study, the modelling was conducted in stages, carefully considering the experimental setup to match the original form of the object under investigation. The research process began with determining the geometry based on the railway spring design, referencing relevant journals. The modelling was then carried out using CAD software Autodesk Inventor 2017, with the generated geometry exported in .stp file format. This geometry was subsequently converted from a solid to a surface model using Ansys software. The modelled spring was simulated using Ansys, employing the Finite Element Analysis (FEA) method. The meshing process was conducted with Ansys software to ensure the accuracy of the simulation. Following this, modal analysis was performed by testing six natural frequency modes, and the results were linked to the harmonic response according to the dynamic scenario set for the study. The simulation results processed by Ansys were then thoroughly analyzed to achieve the objectives of this research.

This comprehensive approach was aimed at giving deep insights into the dynamic performance and durability of 46SiCrMo6 steel springs in locomotive suspensions. It supports the design optimization and reliability improvements. The steps for conducting this research are depicted in Figure 1. It initiated with identification and problem formulation, material preparation according to the properties, and selection of 46SiCrMo6 steel, determining modelling, meshing, boundary conditions, processing modal analysis, obtaining the results, and discussing them.

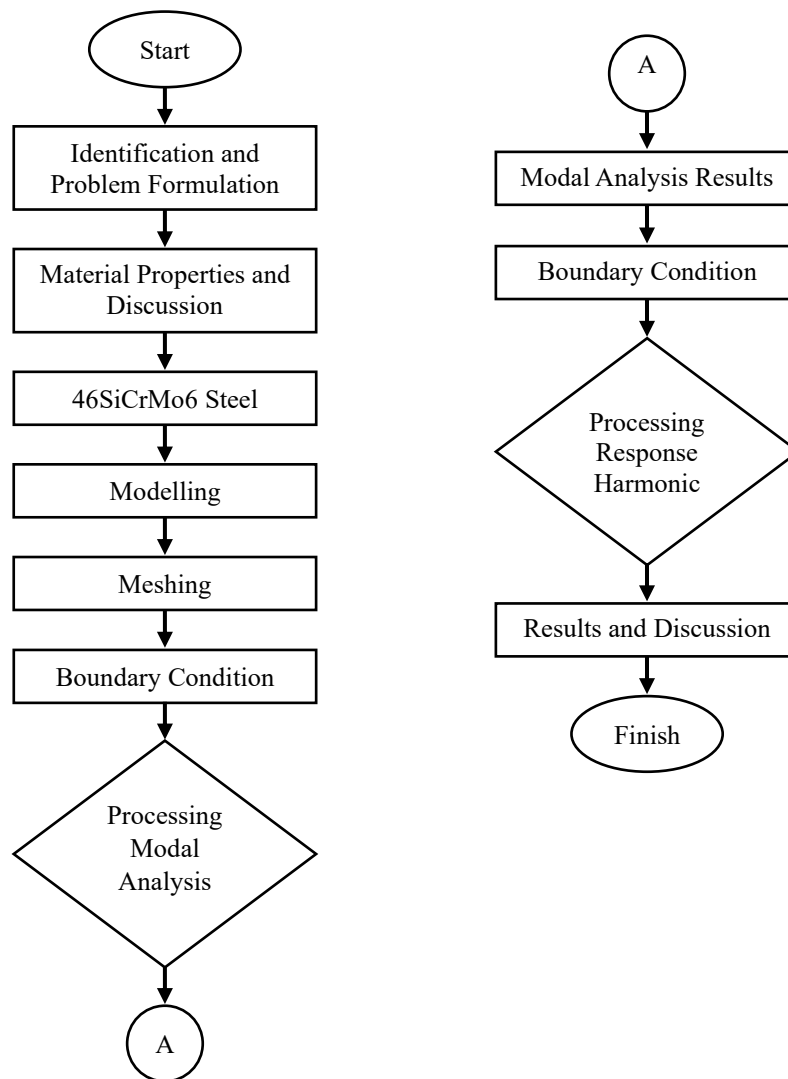


Figure 1. Flowchart of research process

Figure 1 represents the structured research methodology in conducting the research on the dynamic simulation of a locomotive’s primary suspension spring made from 46SiCrMo6 steel. The problem identification and formulation establish the research objective and scope for determining the materials for the locomotive spring. The next step is a discussion of material properties. It focuses on the selected 46SiCrMo6 steel as it has high strength and fatigue resistance properties. The 3D model of the suspension spring is subsequently created to do simulation, and the meshing process is applied to discretize the geometry for finite element analysis. After defining appropriate boundary conditions, the simulation is conducted for modal analysis processing. It is the determination process of natural frequencies and mode shapes of the spring.

The review of modal analysis results is conducted in the next step. It is important to set up the subsequent harmonic response analysis. Another set of boundary conditions is applied to stimulate the constraints and dynamic loading. The harmonic response analysis is a process to evaluate the spring behaviour under varying frequency excitation. It particularly focuses on amplitude and stress response. At last, the results and discussion phase interpret the simulation data.

3. Results and Discussion

In the modal analysis, testing data were obtained across six modes, with each material yielding different results. The six modes provided natural frequency (Hz) and deformation (mm) results as Figure 2.

In Mode 1, as shown in Figure 2 (a), the largest deformation occurred in the middle of the spring with a frequency of 49.785 Hz. In Mode 2, as shown in Figure 2 (b), the largest deformation was observed on the side of the middle spring with a frequency of 55.29 Hz. In Mode 3, as shown in Figure 2 (c), the largest deformation again occurred in the middle of the spring with a frequency of 64.399 Hz. In Mode 4, as shown in Figure 2 (d), the largest deformation was located on the side of the middle spring with a frequency of 64.578 Hz. In Mode 5, as shown in Figure 2 (e), the largest deformation occurred at the top and bottom of the spring with a frequency of 96.269 Hz. In Mode 6, as shown in Figure 2 (f), the largest deformation was again observed on the side of the middle spring with a frequency of 101.76 Hz.

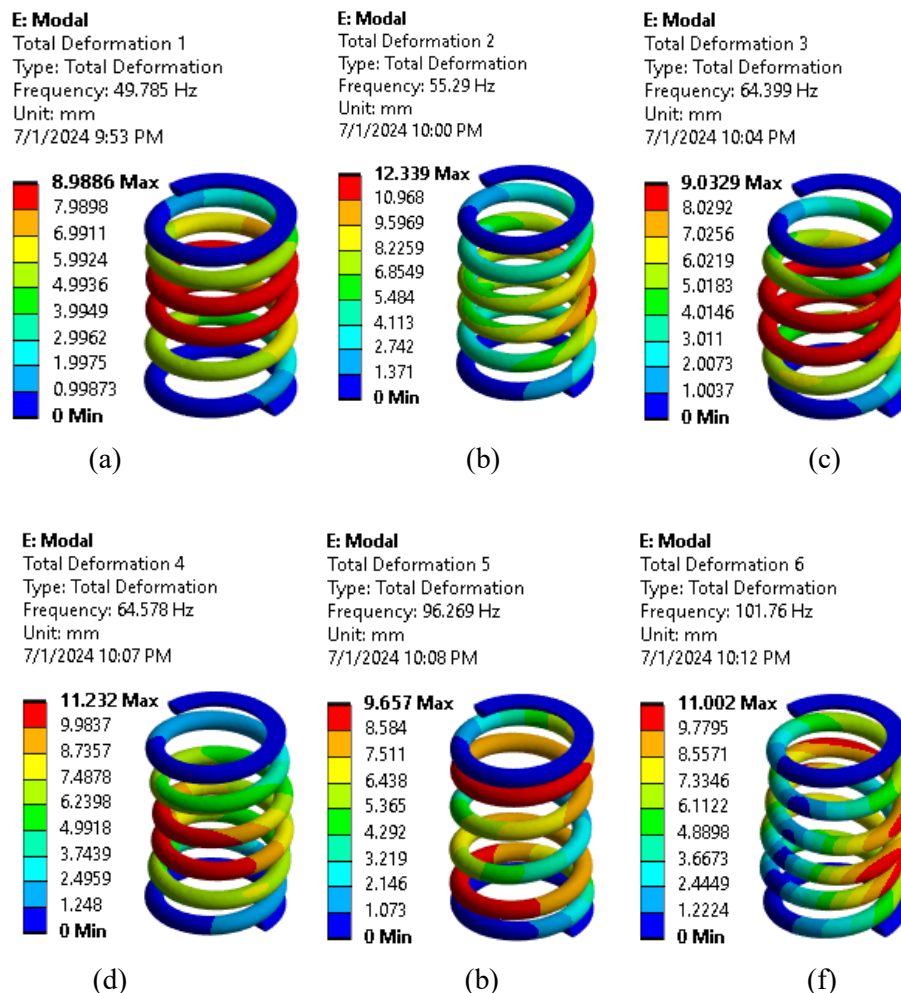


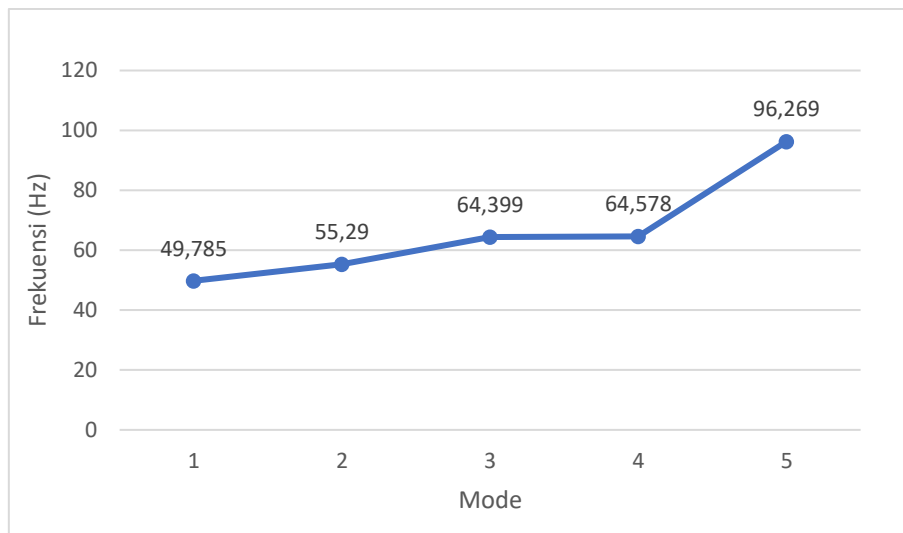
Figure 2. Modes: (a) Mode 1, (b) Mode 2, (c) Mode 3, (d) Mode 4, (e) Mode 5, (f) Mode 6

Once the analysis data were obtained, all the data were grouped by type, as shown in Table 3. Table 3 presents the frequency data for 46SiCrMo6 steel, and deformation data.

Table 1. Frequency data for 46SiCrMo6 steel and deformation

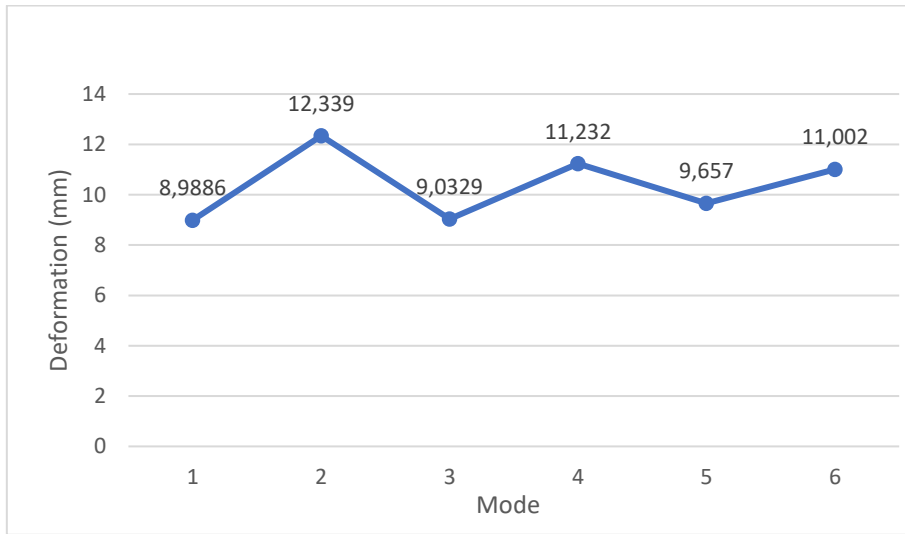
Mode	46SiCrMo6 steel	46SiCrMo6 steel
1	49.785	8.9886
2	55.29	12.339
3	64.399	9.0329
4	64.578	11.232
5	96.269	9.657
6	101.76	11.002

After all the data were categorized, the next step was to analyze the data in the form of a graph, as shown in Graphs 1, 2, 3, and 4.



Graph 1. Frequency Comparison with Material

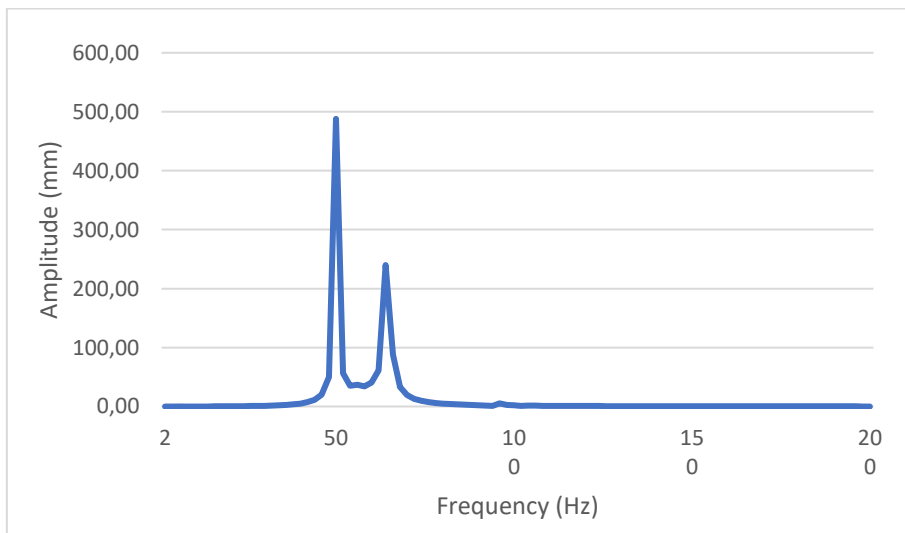
Graph 1 shows that the natural frequency from the modal analysis of the 46SiCrMo6 material tends to increase with each subsequent mode. This graph represents the relationship between vibration mode and the natural frequency, which is determined in Hertz. It is the data of the frequency results of a suspension spring made of 46SiCrMo6 steel. It is commonly used in locomotive applications. The first mode occurs at 49.785 Hz and mode 2 at 55.29 Hz. Meanwhile, modes 3 and 4 have very close values. They are 64.399 Hz and 64.578 Hz, respectively. It indicates the possibility of symmetric vibration patterns. The fifth mode shows a significant incline in frequency to 96.269 Hz. It proposes a higher-order deformation pattern with a more rigid response. This frequency distribution provides essential information for dynamic analysis, as a resonance occurs when excitation frequencies match these natural frequencies.



Graph 2. Deformation Comparison Graph with Material

Graph 1 and 2 show that the maximum deformation in the modal analysis of the 46SiCrMo6 material shows a fluctuating pattern, rising and falling with each mode.

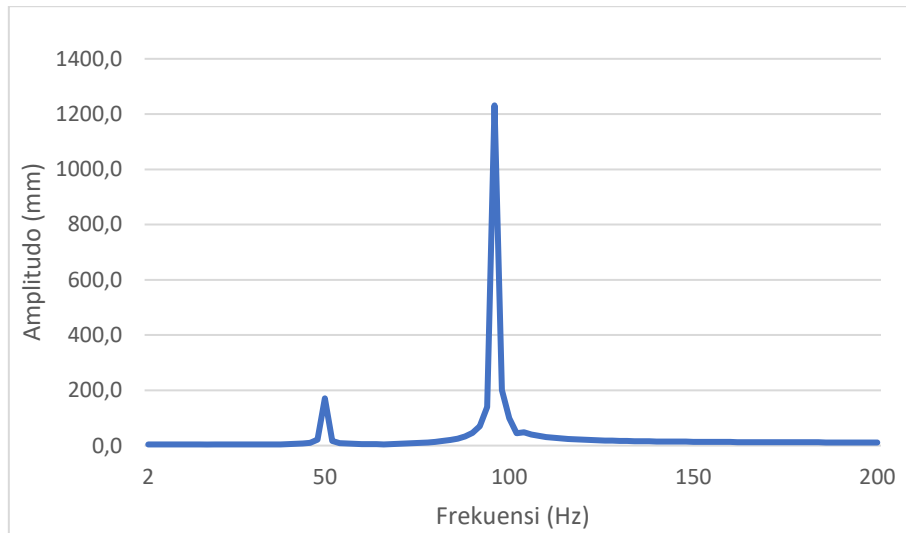
Modal analysis was conducted to identify the natural frequencies and mode shapes of the spring. This is necessary because resonance occurs if the excitation frequency matches one of the natural frequencies, leading to large-amplitude oscillations. Following the modal analysis simulation, the next step was to simulate the harmonic response. This section aims to determine the frequency and amplitude of the material test. The identification of resonant frequencies and the assessment of vibration amplitude were conducted to analyze the output of the harmonic response simulation.



Graph 3. Amplitude vs. Frequency Comparison for Deformation

Graph 3 presents the relationship between amplitude and frequency in the deformation of a primary suspension spring in locomotives. It shows a clear resonance behavior. According to this graph, the highest amplitude was recorded at 487.91 mm with a frequency of 50 Hz. It indicates a strong resonant frequency in the spring where it experiences maximum deformation due to dynamic excitation. The lower peak of the

resonant is at 240 mm, which appears shorter after the first. It offers the presence of another natural frequency or a harmonic. Apart from these peaks, the amplitude reaches almost zero across the remaining frequency range. It shows the drop-off values of amplitude in different frequencies. The decreased values of amplitude in these frequencies indicate that the suspension spring system has less response to frequencies outside the resonant range.



Graph 4. Amplitude vs. Frequency Comparison for Von-Mises Stress

Graph 4 displays the relationship between frequency and amplitude from the Von-Mises stress of the primary suspension spring in the locomotive. The graph shows two different resonance peaks. It indicates frequencies where the spring experiences significant stress amplification due to dynamic excitation. The first peak occurs at 50 Hz with 171.0 mm amplitude. Meanwhile, the highest amplitude was recorded at 1231.5 mm with a frequency of 96 Hz. It represents the primary resonant frequency at which the spring is most vulnerable to stress-induced deformation. Beyond 120 Hz, the amplitude sharply drops off and remains low. It shows the stable behaviour in those areas. The identification of resonant frequencies is important in locomotive suspension design as the operation near this part leads to excessive stress, fatigue, or failure of the suspension spring.

4. Conclusion

In this study, the analysis was conducted on the primary suspension spring of a locomotive to determine the natural frequency through modal analysis, deformation, and von Mises stress in harmonic response analysis. The analysis was carried out using three different materials with the Ansys application, and the conclusions drawn are as follows:

From the modal analysis, it was found that the spring experiences six natural frequency modes, representing the train's condition during bumping and turning. The deformation point on the spring most frequently occurs in the middle coil, where strain causes frequent material failure.

In the modal analysis, the maximum deformation occurred in mode 2 at 12.339 mm, while the highest frequency occurred in mode 6 at 101.76 Hz. Meanwhile, in

harmonic response analysis, the highest amplitude for deformation was recorded at 487.91 mm with a frequency of 50 Hz. Meanwhile, the highest amplitude for von Mises stress was also recorded at 487.91 mm with a frequency of 50 Hz. The dynamic simulation of the spring was conducted using 46SiCrMo6 steel, indicating that further research should be conducted using different materials.

References

- [1] G. Li, S. W. Or, and K. W. Chan, “Intelligent Energy-Efficient Train Trajectory Optimization Approach Based on Supervised Reinforcement Learning for Urban Rail Transits,” *IEEE Access*, vol. 11, pp. 31508–31521, 2023, doi: [10.1109/ACCESS.2023.3261900](https://doi.org/10.1109/ACCESS.2023.3261900).
- [2] M. V Konstantinova, A. A. Olentsevich, V. Y. Konyukhov, E. A. Guseva, and V. A. Olentsevich, “Automation of failure forecasting on the subsystems of the railway transport complex in order to optimize the transportation process as a whole,” *IOP Conf. Ser. Mater. Sci. Eng.*, vol. 1064, no. 1, p. 012020, Feb. 2021, doi: [10.1088/1757-899X/1064/1/012020](https://doi.org/10.1088/1757-899X/1064/1/012020).
- [3] C. Sundling and V. Ceccato, “The impact of rail-based stations on passengers’ safety perceptions. A systematic review of international evidence,” *Transp. Res. Part F Traffic Psychol. Behav.*, vol. 86, pp. 99–120, Apr. 2022, doi: <https://doi.org/10.1016/j.trf.2022.02.011>.
- [4] A. Lovska, O. Fomin, V. Píštěk, and P. Kučera, “Dynamic Load Modelling within Combined Transport Trains during Transportation on a Railway Ferry,” *Appl. Sci.*, vol. 10, no. 16, p. 5710, Aug. 2020, doi: <https://doi.org/10.3390/app10165710>.
- [5] Y. Yao, G. Li, G. Wu, Z. Zhang, and J. Tang, “Suspension parameters optimum of high-speed train bogie for hunting stability robustness,” *Int. J. Rail Transp.*, vol. 8, no. 3, pp. 195–214, Jul. 2020, doi: <https://doi.org/10.1080/23248378.2019.1625824>.
- [6] Y. Han, W. Shi, and W. Feng, “Dynamic Damage Detection and Assessment on the Bogie Frame of High-Speed Train Based on the Coupled Elastic and Multibody Dynamics Scheme,” *Acta Mech. Solida Sin.*, vol. 36, no. 5, pp. 633–646, Oct. 2023, doi: [10.1007/s10338-023-00410-2](https://doi.org/10.1007/s10338-023-00410-2).
- [7] C. Zhang, H. Kordestani, and M. Shadabfar, “A combined review of vibration control strategies for high-speed trains and railway infrastructures: Challenges and solutions,” *J. Low Freq. Noise, Vib. Act. Control*, vol. 42, no. 1, pp. 272–291, Mar. 2023, doi: <https://doi.org/10.1177/14613484221128682>.
- [8] M. Dumitriu, “Condition Monitoring of the Dampers in the Railway Vehicle Suspension Based on the Vibrations Response Analysis of the Bogie,” *Sensors*, vol. 22, no. 9, p. 3290, Apr. 2022, doi: <https://doi.org/10.3390/s22093290>.
- [9] X. Wu, C. Xie, K. Liu, S. Wu, Z. Wen, and J. Mo, “Study on high frequency vibration-induced fatigue failure of antenna beam in a metro bogie,” *Eng. Fail. Anal.*, vol. 133, p. 105976, Mar. 2022, doi: <https://doi.org/10.1016/j.engfailanal.2021.105976>.
- [10] H. Zheng and W. Yan, “Field and numerical investigations on the environmental vibration and the influence of hill on vibration propagation induced by high-speed trains,” *Constr. Build. Mater.*, vol. 357, p. 129378, Nov. 2022, doi: <https://doi.org/10.1016/j.conbuildmat.2022.129378>.
- [11] X. Liu *et al.*, “Measurements and modelling of dynamic stiffness of a railway vehicle primary suspension element and its use in a structure-borne noise transmission model,” *Appl. Acoust.*, vol. 182, p. 108232, Nov. 2021, doi: <https://doi.org/10.1016/j.apacoust.2021.108232>.

- [12] D. Lebel, C. Soize, C. Funfschilling, and G. Perrin, “High-speed train suspension health monitoring using computational dynamics and acceleration measurements,” *Veh. Syst. Dyn.*, vol. 58, no. 6, pp. 911–932, Jun. 2020, doi: <https://doi.org/10.1080/00423114.2019.1601744>.
- [13] B. Fu, R. L. Giossi, R. Persson, S. Stichel, S. Bruni, and R. Goodall, “Active suspension in railway vehicles: a literature survey,” *Railw. Eng. Sci.*, vol. 28, no. 1, pp. 3–35, Mar. 2020, doi: [10.1007/s40534-020-00207-w](https://doi.org/10.1007/s40534-020-00207-w).
- [14] V. Tiwari, S. C. Sharma, and S. P. Harsha, “Ride comfort analysis of high-speed rail vehicle using laminated rubber isolator based secondary suspension,” *Veh. Syst. Dyn.*, vol. 61, no. 10, pp. 2689–2715, Oct. 2023, doi: <https://doi.org/10.1080/00423114.2022.2131584>.
- [15] T. Jin *et al.*, “Development and evaluation of a versatile semi-active suspension system for high-speed railway vehicles,” *Mech. Syst. Signal Process.*, vol. 135, p. 106338, Jan. 2020, doi: <https://doi.org/10.1016/j.ymssp.2019.106338>.
- [16] Y. Ye, Y. Sun, S. Dongfang, D. Shi, and M. Hecht, “Optimizing wheel profiles and suspensions for railway vehicles operating on specific lines to reduce wheel wear: a case study,” *Multibody Syst. Dyn.*, vol. 51, no. 1, pp. 91–122, Jan. 2021, doi: [10.1007/s11044-020-09722-4](https://doi.org/10.1007/s11044-020-09722-4).
- [17] M. A. Kumbhalkar, D. V. Bhope, P. P. Chaoji, and A. V. Vanalkar, “Investigation for Failure Response of Suspension Spring of Railway Vehicle: A Categorical Literature Review,” *J. Fail. Anal. Prev.*, vol. 20, no. 4, pp. 1130–1142, Aug. 2020, doi: [10.1007/s11668-020-00918-6](https://doi.org/10.1007/s11668-020-00918-6).
- [18] F. Guo, S. C. Wu, J. X. Liu, W. Zhang, Q. B. Qin, and Y. Yao, “Fatigue life assessment of bogie frames in high-speed railway vehicles considering gear meshing,” *Int. J. Fatigue*, vol. 132, p. 105353, Mar. 2020, doi: <https://doi.org/10.1016/j.ijfatigue.2019.105353>.